Langmuir
Article
pubs.acs.org/Langmuir

Tuning the Magnetic Resonance Imaging Properties of Positive Contrast Agent Nanoparticles by Surface Modification with RAFT Polymers

Misty D. Rowe,[†] Chia-Chih Chang,[†] Douglas H. Thamm,[‡] Susan L. Kraft,[‡] Joseph F. Harmon, Jr.,[‡] Andrew P. Vogt,[§] Brent S. Sumerlin,[§] and Stephen G. Boyes*,[†]

[†]*Department of Chemistry and Geochemistry, Colorado School of Mines, Golden, Colorado 80401,* [‡]*College of Veterinary Medicine and Biological Sciences, Animal Cancer Center, Colorado State University, Fort Collins, Colorado 80526, and* [§]*Department of Chemistry, Southern Methodist University, Dallas, Texas 75275*

Received March 1, 2009. Revised Manuscript Received April 6, 2009

A novel surface modification technique was employed to produce a polymer modified positive contrast agent nanoparticle through attachment of well-defined homopolymers synthesized via reversible addition−fragmentation chain transfer (RAFT) polymerization. A range of RAFT homopolymers including poly[*N*-(2-hydroxypropyl) methacrylamide], poly(*N*-isopropylacrylamide), polystyrene, poly(2-(dimethylamino)ethyl acrylate), poly(((poly)ethylene glycol) methyl ether acrylate), and poly(acrylic acid) were synthesized and subsequently used to modify the surface of gadolinium (Gd) metal−organic framework (MOF) nanoparticles. Employment of a trithiocarbonate RAFT agent allowed for reduction of the polymer end groups under basic conditions to thiolates, providing a means of homopolymer attachment through vacant orbitals on the Gd^{3+} ions at the surface of the Gd MOF nanoparticles. Magnetic resonance imaging (MRI) confirmed the relaxivity rates of these novel polymer modified structures were easily tuned by changes in the molecular weight and chemical structures of the polymers. When a hydrophilic polymer was used for modification of the Gd MOF nanoparticles, an increase in molecular weight of the polymer provided a respective increase in the longitudinal relaxivity. These relaxivity values were significantly higher than both the unmodified Gd MOF nanoparticles and the clinically employed contrast agents, Magnevist and Multihance, which confirmed the construct's ability to be utilized as a positive contrast nanoparticle agent in MRI. Further characterization confirmed that increased hydrophobicity of the polymer coating on the Gd MOF nanoparticles yielded minimal changes in the longitudinal relaxivity properties but large increases in the transverse relaxivity properties in the MRI.

Introduction

Recently, research into the use of inorganic and organometallic nanoparticles has shown great promise in regards to the utilization of these structures in nanosized diagnostic devices. Due to their inherent optical properties, many nanoparticles have demonstrated the ability to be useful for molecular imaging in both a research and clinical setting. For example, superparamagnetic iron oxide (SPIO) nanoparticles and gadolinium (Gd)-based nanoparticles behave as negative and positive contrast agents, respectively, in magnetic resonance imaging (MRI), quantum dots have been utilized as markers in fluorescent microscopy, while gold nanorods have been employed in dark field and confocal microscopy.[1−12] The use of nanoparticles as the imaging agent for diagnostic imaging is beneficial due to the fact that there is a large concentration of imaging agent per particle and these particles have been shown to have longer retention times *in vivo*. However, in order to produce a nanoparticle-based imaging agent that can be easily translated to clinical application, it is important that the nanodevice be useful for application with common and widely utilized diagnostic imaging instrumentation, such as MRI, and can be modified so as to render the nanostructure biocompatible.

Most of the focus on nanoparticle contrast agents for MRI has been on the use of negative contrast SPIOs, with various oral agents being already approved for clinical use (Ferumoxsil, Ferumoxide) and others being in clinical phases II and III (Ferucarbotran, Ferumoxtran). However, negative contrast agents suffer from a series of drawbacks, including MRI cannot distinguish the void from the contrast agent from other signal voids, negative contrast agents are limited by partial volume effects, and tracking cells *in vivo* can be difficult. Recently, focus on nanoparticle-based MRI contrast agents has shifted to Gd-based nanoparticles due to their ability to act as a positive contrast agent and their relationship to currently employed MRI contrast agents, such as Magnevist and Multihance, which are based on Gd chelates. This attention on Gd-based nanoparticles has been mostly driven by limitations with the conventional contrast agents based on Gd chelates, such as a low concentration of Gd per molecule, short retention times *in vivo* due to contrast agent dimensions, limited biostability, and difficulty in functionalization to enable use in more complex diagnostic devices.

*Corresponding author. E-mail: sboyes@mines.edu.

(1) Huang, X.; El-Sayed, I. H.; Qian, W.; El-Sayed, M. A. *J. Am. Chem. Soc.* **2006**, *128*, 2115–2120.
(2) Rieter, W. J.; Taylor, K. M. L.; An, H.; Lin, W.; Lin, W. *J. Am. Chem. Soc.* **2006**, *128*, 9024–9025.
(3) Rieter, W. J.; Taylor, K. M. L.; Lin, W. *J. Am. Chem. Soc.* **2007**, *129*, 9852–9853.
(4) Taboada, E.; Rodriquez, E.; Roig, A.; Oro, J.; Roch, A.; Muller, R. N. *Langmuir* **2007**, *23*, 4583–4588.
(5) Oyewumi, M. O.; Mumper, R. J. *Drug Dev. Ind. Pharm.* **2002**, *28*, 317–328.
(6) Oyewumi, M. O.; Mumper, R. J. *Bioconjugate Chem.* **2002**, *13*, 1328–1335.
(7) Oyewumi, M. O.; Liu, S.; Moscow, J. A.; Mumper, R. J. *Bioconjugate Chem.* **2003**, *14*, 404–411.
(8) Oyewumi, M. O.; Yokel, R. A.; Jay, M.; Coakley, T.; Mumper, R. J. *J. Controlled Release* **2004**, *95*, 613–626.
(9) Oyewumi, M. O.; Mumper, R. J. *Int. J. Pharm.* **2003**, *251*, 85–97.
(10) Bridot, J.-L.; Faure, A.-C.; Laurent, S.; Riviere, C.; Billotey, C.; Hiba, B.; Jainer, M.; Josserand, V.; Coll, J.-L.; Vander Elst, L.; Muller, R.; Roux, S.; Perriat, P.; Tillement, O. *J. Am. Chem. Soc.* **2007**, *129*, 5076–5084.
(11) Evanics, F.; Diamente, P. R.; van Veggel, F. C. J. M.; Stanisz, G. J.; Prosser, R. S. *Chem. Mater.* **2006**, *18*, 2499–2505.
(12) Rosi, N. L.; Mirkin, C. A. *Chem. Rev.* **2005**, *105*, 1547–1562.

These Gd-based nanoparticles have been synthesized with both inorganic and organometallic compounds of Gd such as gadolinium oxide, gadolinium phosphate, gadolinium fluoride, gadolinium hexanedione and acetylacetenoate mixed with emulsifying wax, and most recently nanoscale metal−organic frameworks (MOFs).[2,3,5−11,13] While Gd-based nanoparticles exhibit relaxivities significantly higher than those of typical Gd chelates and also provide a contrast agent with higher molecular weights for improved retention times and a high concentration of Gd^{3+} ions per contrast agent particle, their application has been limited due to the difficulty in producing nanoparticles that are biocompatible and stable, and have specific surface functionality.[3,13]

Due to the tremendous potential of Gd nanoparticles as nanoscale contrast agents for MRI, researchers have attempted to overcome some of their inherent limitations by developing methods to surface modify the nanoparticles.[6−8] To date, these surface modification methods have demonstrated limited success, as they have resulted in poorly defined surfaces with a lack of control over the surface functionality, instabilities in the coatings due to their noncovalent nature, or reduced imaging capabilities due to masking of the underlying Gd nanoparticle. As such, the search for a surface modification technique that provides control over surface functionality and architecture, along with the ability to produce a stable structure without diminishing the inherent imaging properties, represents a significant challenge for researchers. One of the most interesting Gd nanoparticle systems are the nanoscale MOFs, which are constructed from Gd^{3+} ions and organic bridging ligands, such as 1,4-benzenedicarboxylic acid (1,4-BDC), as they have demonstrated exceptional MRI capabilities.[2,14,15] Surface modification of Gd-based MOFs through covalent attachment of well-defined polymers offers a means of modifying and/or tuning the relaxation properties of the nanoparticles, incorporating a higher degree of functionality and increasing the *in vivo* stability and biocompatibility.

Reversible addition−fragmentation chain transfer (RAFT) polymerization is arguably the most versatile living radical polymerization (LRP) technique with respect to monomer choice and its functional group tolerance. It has been widely employed for the preparation of highly specialized materials for advanced biomedical applications, such as antibody and small interfering ribonucleic acid polymer conjugates, controlled drug delivery vehicles, and bioconjugation.[16−22] Due to the well-defined nature of the RAFT polymerization technique, another advantage of RAFT polymers is the presence of a thiocarbonylthio group on the end of each polymer chain. Literature has shown that the thiocarbonylthio end groups can be reduced to a thiol in the presence of a nucleophile, such as a primary amine or sodium borohydride.[23,24] Because thiols have been shown to react strongly with a variety of metal surfaces, such as gold and silver, and the surface of semiconducting nanoparticles, such as CdSe nanoparticles, RAFT polymerization is uniquely placed as one of the premier polymerization techniques to prepare polymers for surface functionalization of a wide range of both planar and nanoparticle substrates.[23−26] Currently, there are no reports of the utilization of the RAFT polymerization technique to produce well-defined polymers that allow for the surface modification of Gd MOF nanoparticles to produce polymer modified positive contrast nanoparticle agent platforms for MRI. Herein, Gd MOF nanoparticles were synthesized by a procedure discussed previously in the literature.[2] A novel surface modification procedure was developed allowing the attachment of well-defined polymers synthesized via RAFT polymerization through reduction of the thiocarbonylthio end group under basic conditions to form thiolates and further attachment through coordination chemistry to the Gd MOF nanoparticles (Scheme 1). Furthermore, *in vitro* MRI was employed to determine the relaxivities of the novel polymer modified Gd MOF nanoparticles in comparison to the clinically employed contrast agents, Magnevist and Multihance. Finally, tailoring the functionality and thickness of the polymer coating provided a means of tuning the MRI characteristics of these novel polymer modified positive contrast nanoparticle agents.

Experimental Section

Materials. *N*-Isopropylacrylamide (NIPAM) (97%), 2-(dimethylamino)ethyl acrylate (DMAEA) (stabilized with 1000 ppm monomethyl ether of hydroquinone (MEHQ)) (98%), poly (ethylene glycol) methyl ether acrylate (PEGMEA) (average $M_n \sim 454$ g/mol, stabilized with 100 ppm MEHQ and 300 ppm butylated hydroxytoluene), anhydrous 1,4-dioxane (99.8%), anhydrous toluene (99.8%), anhydrous tetrahydrofuran (THF) (>99.9%), 2,2-azobisisobutyronitrile (AIBN) (98%), anhydrous methanol, carbon disulfide (ACS reagent), tetrabutylammonium bromide (99%), gadolinium(III) chloride ($GdCl_3$) (99.999%), terephthalic acid (98%), hexyl alcohol (98%), methylamine solution (40 wt % in water), cetyltrimethylammonium bromide (CTAB) (Sigma Ultra, ∼99%), 1-amino-2-propanol (93%), *N*-hydroxysuccinimide (98%), triethylamine (99.5%), and 1-dodecanethiol (98+%) were purchased from Sigma-Aldrich. Styrene (Sty) (stabilized with 10−15 ppm *tert*-butylcatechol) (99%), acrylic acid (AA) (stabilized with 200 ppm MEHQ, 99.5%), anhydrous *N*,*N*-dimethylformamide (DMF) (99.8%), hexylamine (99%), and tricaprylyl methylammonium chloride (Aliquot 336) were purchased from Acros. Methacryloyl chloride (≥97%) and dichloromethane (absolute, over molecular sieve, $H_2O \leq 0.005\%$) were purchased from Fluka. Heptane (HPLC), hexanes (HPLC), acetone (reagent grade), isopropyl alcohol (reagent grade), ethyl acetate (HPLC), sodium sulfate (anhydrous, granular, 10−60 mesh), and DMF (HPLC) were purchased from Mallinckrodt Chemicals. Deionized ultrafiltered (DIUF) water, chloroform (HPLC), hydrochloric acid (reagent), and sodium hydroxide were purchased from Fisher. Triethylamine was distilled under pressure and stored in the freezer prior to use. NIPAM was doubly recrystallized from hexanes before use. AIBN was doubly recrystallized from methanol prior to use. Sty was filtered over basic alumina oxide and then stored in a freezer prior to use. AA, DMAEA, and PEGMEA were distilled under vacuum and then stored in a freezer prior to use. All other chemicals, unless otherwise discussed, were reagent grade and used as received.

(13) Hifumi, H.; Yamaoka, S.; Tanimoto, A.; Citterio, D.; Suzuki, K. *J. Am. Chem. Soc.* **2006**, *128*, 15090–15091.
(14) James, S. *Chem. Soc. Rev.* **2003**, *32*, 276–288.
(15) Taylor, K. M. L.; Kim, J. S.; Rieter, W. J.; An, H.; Lin, W.; Lin, W. *J. Am. Chem. Soc.* **2008**, *130*, 2154–2155.
(16) Yanjarappa, M. J.; Gujraty, K. V.; Joshi, A.; Saraph, A.; Kane, R. S. *Biomacromolecules* **2006**, *7*, 1665–1670.
(17) Hong, C.-Y.; Pan, C.-Y. *Macromolecules* **2006**, *39*, 3517–3524.
(18) Nguyen, T. L.; Tey, S. Y.; Pourgholami, M. H.; Morris, D. L.; Davis, T. P.; Barner-Kowollik, C.; Stenzel, M. H. *Eur. Polym. J.* **2007**, *43*, 1754–1767.
(19) Scales, C. W.; Huang, F.; Li, N.; Vasilieva, Y. A.; Ray, J.; Convertine, A. J.; McCormick, C. L. *Macromolecules* **2006**, *39*, 6871–6881.
(20) Zelikin, A. N.; Such, G. K.; Postma, A.; Caruso, F. *Biomacromolecules* **2007**, *8*, 2950–2953.
(21) Li, M.; De, P.; Gondi, S. R.; Sumerlin, B. S. *Macromol. Rapid Commun.* **2008**, *29*, 1172–1176.
(22) De, P.; Li, M.; Gondi, S. R.; Sumerlin, B. S. *J. Am. Chem. Soc.* **2008**, *130*, 11288–11289.
(23) Sumerlin, B. S.; Lowe, A. B.; Stroud, P. A.; Zhang, P.; Urban, M. W.; McCormick, C. L. *Langmuir* **2003**, *19*, 5559–5562.
(24) Hotchkiss, J. W.; Lowe, A. B.; Boyes, S. G. *Chem. Mater.* **2007**, *19*, 6–13.
(25) Zhang, Q.; Gupta, S.; Emrick, T.; Russell, T. P. *J. Am. Chem. Soc.* **2006**, *128*, 3898–3899.
(26) Lowe, A. B.; Sumerlin, B. S.; Donovan, M. S.; McCormick, C. L. *J. Am. Chem. Soc.* **2002**, *124*, 11562–11563.

Scheme 1. General Route for the Modification of Gadolinium Metal−Organic Framework Nanoparticles with Homopolymers Synthesized by RAFT Polymerization

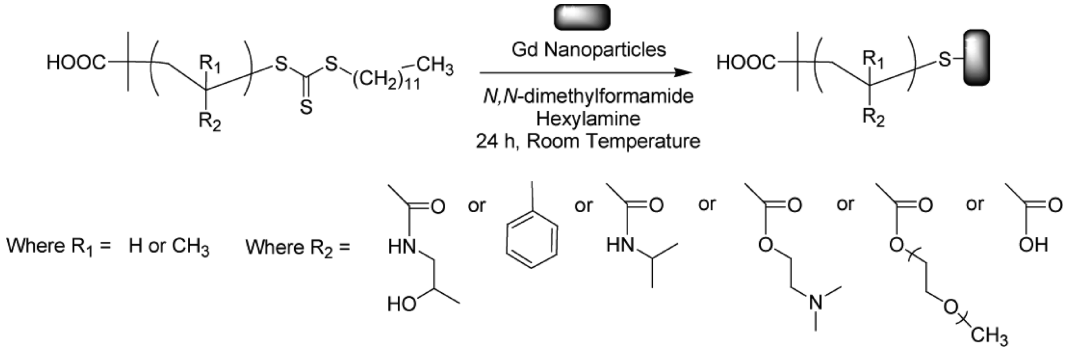

Synthesis of *S*-1-Dodecyl *S*′-(α,α-Dimethylacetic acid) Trithiocarbonate (DATC). DATC was prepared via Lai et al.'s literature procedure.[27] ^{1}H NMR (60 MHz, $CDCl_3$, δ, ppm): 0.89 (t, 3H), 1.25−1.53 (m, 20H), 1.73 (s, 6H), 3.35 (t, 2H). FTIR (cm^{-1}): 1702 (C═O), 1065 (C═S).

Synthesis of *N*-(2-Hydroxypropyl) Methacrylamide (HPMA). HPMA was synthesized by a procedure in the literature.[28] Briefly, 1-amino-2-propanol (45.5 mL, 0.589 mol) and ethyl acetate (450 mL) were added to a 1 L two-neck round-bottom flask equipped with an overhead automatic stirrer and a 100 mL addition funnel. The flask was then cooled to −10 °C and purged with high-purity nitrogen gas for 15 min and then left under a nitrogen atmosphere. Ethyl acetate (50 mL) and methacryloyl chloride (28 mL, 0.287 mol) were added to the addition funnel. The addition funnel was then sealed and purged with high-purity nitrogen gas for 15 min and left under a nitrogen atmosphere. The ethyl acetate/methacryloyl chloride mixture was then added dropwise to the ethyl acetate/1-amino-2-propanol mixture. Once the addition was complete, the reaction flask was transferred to an ice bath for 1 h. The reaction mixture was then allowed to warm to room temperature, after which a saturated solution of sodium sulfate in DIUF water (250 mL) was added. The reaction solution was then transferred to a separatory funnel and washed, discarding the aqueous layer. Two to three subsequent washes with saturated sodium sulfate solution allowed for complete removal of any excess reactants and side products. The organic layer was then dried over sodium sulfate for 12 h and then concentrated via rotary evaporation to approximately 30 mL. The concentrate was then allowed to age for 1 h at −10 °C. The product was then collected by filtration, dried under vacuum, and stored in the freezer prior to use (12.0 g, percent yield = 30%). ^{1}H NMR (60 MHz, $CDCl_3$, δ, ppm): 1.21 (d, 3H), 1.98 (s, 3H), 3.19 (t, 1H), 3.50 (d, 1H), 3.90 (d, 2H), 5.35 (s, 1H), 5.75 (s, 1H), 6.42 (br, 1H). FTIR (cm^{-1}): 3275 (−OH), 3095 (−NH−), 2980 and 2925 (CH═CH_2), 1650 (NH−C═O).

Homopolymer Formation via RAFT Polymerization. The general polymerization procedure to form homopolymers via RAFT polymerization involved the addition of monomer, RAFT agent, and solvent, as needed, to a 150 mL Schlenk flask. The solution was degassed for 30 min and then left under a high purity nitrogen atmosphere. AIBN was added to a second 150 mL Schlenk flask. The second flask was sealed with a septum, subjected to three evacuation−purge cycles, and then left under a high purity nitrogen atmosphere. The monomer solution was then transferred via cannula to the initiator containing flask, and the reaction was heated for a set amount of time. Polymer from the polymerization solution was isolated by evaporating residual monomer and solvent under vacuum overnight.

Specific RAFT polymerization conditions per monomer are as follows: **HPMA** (6.00 g, 4.17×10^{-2} mol), *tert*-butanol (40.0 mL), DATC (0.100 g, 2.82×10^{-4} mol), AIBN (0.00450 g, 2.74×10^{-5} mol), 80 °C, 2.5 h (conversion = 22.8%, $M_{n,theoretical}$ = 5,129 g/mol, $M_{n,experimental}$ = 5,327 g/mol). **HPMA** (6.00 g, 4.17×10^{-2} mol), *tert*-butanol (40.0 mL), DATC (0.100 g, 2.82×10^{-4} mol), AIBN (0.00450 g, 2.74×10^{-5} mol), 80 °C, 5 h (conversion = 41.5%, $M_{n,theoretical}$ = 9,073 g/mol, $M_{n,experimental}$ = 10 281 g/mol). **HPMA** (8.50 g, 5.90×10^{-2} mol), *tert*-butanol (40.0 mL), DATC (0.100 g, 2.82×10^{-4} mol), AIBN (0.00450 g, 2.74×10^{-5} mol), 80 °C, 4 h (conversion = 62.4%, $M_{n,theoretical}$ = 19,696 g/mol, $M_{n,experimental}$ = 19 370 g/mol). **NIPAM** (10.07 g, 8.90×10^{-2} mol), DMF (50 mL), DATC (0.488 g, 1.34×10^{-3} mol), AIBN (0.0204 g, 1.24×10^{-4} mol), 60 °C, 1 h (conversion = 73%, $M_{n,theoretical}$ = 5500 g/mol, $M_{n,experimental}$ = 5,690 g/mol). **NIPAM** (6.53 g, 5.77×10^{-2} mol), DMF (25 mL), DATC (0.269 g, 7.38×10^{-4} mol), AIBN (0.0290 g, 1.77×10^{-4} mol), 60 °C, 12 h (conversion = 96%, $M_{n,theoretical}$ = 8733 g/mol, $M_{n,experimental}$ = 8606 g/mol). **NIPAM** (10.07 g, 8.90×10^{-2} mol), DMF (50 mL), DATC (0.0698 g, 1.91×10^{-4} mol), AIBN (0.0290 g, 9.57×10^{-6} mol), 60 °C, 24 h (conversion = 33%, $M_{n,theoretical}$ = 17 109 g/mol, $M_{n,experimental}$ = 17 846 g/mol). **Sty** (18.5 mL, 1.61×10^{-1} mol), anhydrous DMF (7.00 mL), DATC (0.319 g, 8.75×10^{-4} mol), AIBN (0.0279 g, 1.70×10^{-4} mol), 80 °C, 4.5 h (conversion = 25.8%, $M_{n,theoretical}$ = 4938 g/mol, $M_{n,experimental}$ = 4802 g/mol). **Sty** (22.0 mL, 1.91×10^{-1} mol), anhydrous DMF (7.00 mL), DATC (0.200 g, 5.49×10^{-4} mol), AIBN (0.0180 g, 1.10×10^{-4} mol), 80 °C, 4.5 h (conversion = 24.8%, $M_{n,theoretical}$ = 9378 g/mol, $M_{n,experimental}$ = 8972 g/mol). **Sty** (22.0 mL, 1.91×10^{-1} mol), anhydrous DMF (7.00 mL), DATC (0.200 g, 5.49×10^{-4} mol), AIBN (0.0180 g, 1.10×10^{-4} mol), 80 °C, 48 h (conversion = 51.2%, $M_{n,theoretical}$ = 18 928 g/mol, $M_{n,experimental}$ = 15 245 g/mol). **DMAEA** (10 mL, 6.50×10^{-1} mol), anhydrous toluene (12 mL), DATC (0.1500 g, 4.12×10^{-4} mol), AIBN (0.0036 g, 5.50×10^{-5} mol), and 60 °C, 12 h (conversion = 76%, $M_{n,theoretical}$ = 17 451 g/mol, $M_{n,experimental}$ = 15 120 g/mol). **PEGMEA** (12.8 mL, 3.08×10^{-2} mol), anhydrous dioxane (13.5 mL), DATC (0.096 g, 2.64×10^{-4} mol), AIBN (0.0024 g, 1.50×10^{-5} mol), 60 °C, 24 h (conversion = 49%, $M_{n,theoretical}$ = 25 920 g/mol, $M_{n,experimental}$ = 19 542 g/mol). **AA** (20.0 mL, 0.294 mol), DMF (45.5 mL), DATC (0.762 g, 2.10×10^{-3} mol), AIBN (0.0343 g, 2.10×10^{-4} mol), 60 °C, 24 h (conversion = 94%, $M_{n,theoretical}$ = 14 335 g/mol, $M_{n,experimental}$ = 10 888 g/mol).

Formation of Gd MOF Nanoparticles. Gd MOF nanoparticles were synthesized via a reverse microemulsion system developed by Reiter and co-workers employing 0.05 M $GdCl_3$, 0.05 M CTAB, as the surfactant, and 0.075 M 1,4-benzenedicarboxylic acid methyl ammonium salt (1,4-BDC), as the binding ligand.[2] A water to surfactant ratio of 10:1 was utilized to provide nanoplatelet shapes with an average of 53 ± 12 nm in width and 122 ± 30 nm in length. After 24 h, the microemulsion was centrifuged at 5000 rpm for a total of 80 min. After removal of the supernatant, the particles were washed

(27) Lai, J. T.; Filla, D.; Shea, R. *Macromolecules* **2002**, *35*, 6754–6756.
(28) Kopecek, J.; Bazilova, H. *Eur. Polym. J.* **1973**, *9*, 7–14.

with ethanol (15 mL), sonicated, and then recentrifuged for 30 min. The supernatant was discarded. The particles underwent an additional cycle of dispersement in ethanol (15 mL), sonication, and centrifugation to remove any excess reactants. The nanoparticle solution was resuspended in ethanol and then allowed to dry.

Surface Modification of Gd MOF Nanoparticles with RAFT Polymers. In a typical experiment, one of the RAFT homopolymers (0.1 g), discussed above, was added to 25 mL of anhydrous *N*,*N*-dimethylformamide (DMF) in a 150 mL Schlenk flask equipped with a stir bar and then sealed with a rubber septum. The RAFT homopolymer solution was purged with high purity nitrogen and then subsequently left under a nitrogen atmosphere. The RAFT agent terminated homopolymer was then converted to a thiolate terminated homopolymer, through aminolysis, by the addition of 0.075 M hexylamine (0.45 mL) and stirring for 1 h at room temperature. Gd MOF nanoparticles (0.01 g) were suspended in an additional 25 mL of DMF in a second 150 mL Schlenk flask equipped with a stir bar and then sealed with a rubber septum. The nanoparticle solution was then purged with high purity nitrogen for 30 min and was subsequently left under a nitrogen atmosphere. The homopolymer solution was then transferred via cannula to the Gd MOF nanoparticle solution. The resulting solution was allowed to stir for 24 h at room temperature under a nitrogen atmosphere. Untethered polymer was removed from the polymer modified Gd MOF nanoparticles through repeated centrifugation and resuspension in DMF (2×) and ethanol (2×), followed by drying.

Surface Modification of Gd MOF Nanoparticles with Dodecanethiolate. The above Gd MOF nanoparticle surface modification method was used with the exception that dodecanethiol (1.00 mL, 4.17×10^{-3} mol) was used instead of the RAFT homopolymer.

***In Vitro* Relaxivity through Measurements by MRI.** Preliminary characterization of the relaxation properties of the unmodified Gd MOF nanoparticles and RAFT homopolymer modified Gd MOF nanoparticles was accomplished through longitudinal relaxation time (T1) and transverse relaxation time (T2) relaxation measurements made *in vitro* with a direct comparison to the clinically utilized contrast agents, Magnevist and Multihance. Measurements were made on a 1.5 T scanner. Scanning for T1 calculations were done by spin echo imaging using repetition time (TR) values of 10 000, 5000, 2500, 1000, 500, 250, 150, 100, 50, 30, and 25 ms and minimum echo time (TE), 5 nm slice thickness, 128 × 128 matrix and 18 cm field of view. Scanning for T2 calculations were done by spin echo imaging using TR of 1500 and four different TE values of 15, 30, 45, and 60 ms, 5 nm slice thickness, 128 × 128 matrix and 18 cm field of view. All samples, including standard contrast agents, were serially diluted in deionized ultrafiltered water, degassed with high purity nitrogen, and sealed in polypropylene vials. Analysis was performed by acquiring signal intensity (I) measurements via region-of-interest analysis of the samples for all pulse sequences with T1 and T2 values being calculated using: $I_i = I_{o,I}\,(1 - \exp^{(-t/T_i)})$.

Characterization. Attenuated total reflectance Fourier transform infrared (ATR-FTIR) spectra were collected utilizing a Smart SAGA attachment coupled with a Thermo-Electron Nicolet 4700 spectrometer, collecting 16 background scans and 64 sample scans, and utilizing Nicolet's OMNIC software. ^{1}H NMR spectra of the polymers were obtained on a Chemagnetics CMX Infinity 400 solids/liquids NMR spectrometer, and data obtained were manipulated in Galactic GRAMS AI software. Sample concentrations were 5% (w/v) in either deuterated chloroform or DMSO containing 1% TMS as an internal reference. Transmission electron microscopy (TEM) was performed on a Philips CM200 with an accelerating voltage of 120 kV. A Keen View Soft Imaging system coupled to iTEM Universal TEM Imaging Platform software was utilized to acquire digital TEM images. Scanning electron microscopy (SEM) was performed using an accelerating voltage of 8 kV on a JEOL JSM-7000F instrument equipped with an in-lens thermal field emission gun. 2θ powder X-ray diffraction (XRD) pattern was recorded using the Cu Kα line of a Siemens Kristalloflex 81 XRD instrument with 2θ increments of 0.5° and measurements being between 8° and 70° with an internal alumina standard for calibration. Molecular weight analysis was performed utilizing gel permeation chromatography (GPC) with THF or DMF as the eluent. The system comprised a Viscotek 270max system with three ViscoGel columns with a linear range of molecular weights from 20K (g/mol) to 10M (g/mol) connected in series. The THF GPC is a triple detector system comprising an Eldex column heater model CH-150 (30 °C), a Viscotek differential viscometer/low angle laser light scattering detector (model 270, λ = 670 nm, 3 mW laser, detector angles of 7° and 90°), UV/vis detector (model 3210, λ = 254 nm, tungsten/deuterium lamp), and a refractive index detector model 3580 (10 mV, λ = 660 nm). ChromAR grade THF was used as eluent at a flow rate of 1.0 mL/min. PSty samples were dissolved in ChromAR grade THF (5 mg/mL) and were injected using a variable injection volume autosampler. Molecular weight data analysis collected in THF was performed using Viscotek OmniSEC software. Similarly, GPC employing DMF (0.02 M LiBr) as the eluent utilized the same Viscotek components with two ViscoGel I-Series mixed bed columns, G-3000 and G-4000, and samples were run at 60 °C. PNIPAM samples were dissolved in chromatography grade DMF (5 mg/mL) and were injected using a variable injection volume autosampler. The refractive index increment (dn/dc) for PSty was 0.185 mL/g.[29] A dn/dc value of 0.077 mL/g, which was calculated by the instrument, was used for the PNIPAM samples. Both organic GPCs were standardized using PSty (98 000 and 250 000 g/mol) and PMMA (75 000 and 150 000 g/mol) standards. Aqueous GPC was employed using SynChropak CATSEC columns (100, 300, and 1000 Å; Eichrom Technologies Inc.) and 1 wt % acetic acid/0.1 M Na_2SO_4(aq) as the eluent at a flow rate of 0.25 mL/min for the PDMAEA and PHPMA samples. dn/dc values of 0.160 mL/g and 0.176 mL/g, which were calculated by the instrument, were employed for the PDMAEA and PHPMA samples, respectively. PDMAEA and PHPMA samples were dissolved in the eluent at a concentration of 20 mg/mL. Detection was achieved with a Spectra-Physics 2000 detector and an Optilab DST RI detector at ambient temperature and a Wyatt DAWN DSP multiangle laser light scattering detector (λ = 633 nm). Molecular weight data for the PAA samples were obtained on a Viscotek model 302 TDA apparatus at 60 °C, employing a Tosoh Alpha-M column set and *N*,*N*-dimethylsulfoxide (DMSO) salted with 0.05 M LiBr as the mobile phase. The instrument was calibrated against a Pullulan P200 with a literature dn/dc value of 0.06 mL/g and was compared against a dextran T70 standard as verification of the dn/dc, M_w, and recovery. The PAA sample employed a dn/dc value of 0.08 mL/g and was made up at 6 mg/mL. The PAA (30 mg) was first diluted in DMSO (5 mL) and placed inside the TDA apparatus at 60 °C for 20 min, then removed and cooled for 10 min, and finally filtered with a 0.2 μm filter before being injected. Matrix assisted laser desorption ionization time-of-flight mass spectrometry (MALDI-ToF MS) was also employed in the experimental molecular weight determination of PAA samples. The PAA samples were prepared at 5 mg/mL in deionized ultrafiltered water in a sinapinic acid matrix at a mole ratio of 10^{-3}.[30] Measurements were performed using a Voyager-DE STR Applied Biospectromety Workstation MALDI-TOF MS setup with a triple frequency Nd:YAG laser using negative ion analysis in linear mode with a 200 ns delay, at 25 kV, and 85% grid voltage. UV−vis spectroscopy was performed on a Thermo Electron Corp., Nicolet Evolution 300 BB spectrophotometer with a xenon lamp and utilized standard 10 mm quartz cuvettes. Thermal

(29) Michielsen, S. *Polymer Handbook*, 4th ed.; John Wiley & Sons: New York, 1999.

(30) Danis, P. O.; Karr, D. E.; Mayer, F.; Holle, A.; Watson, C. H. *Org. Mass Spectrom.* **1992**, *27*, 843–846.

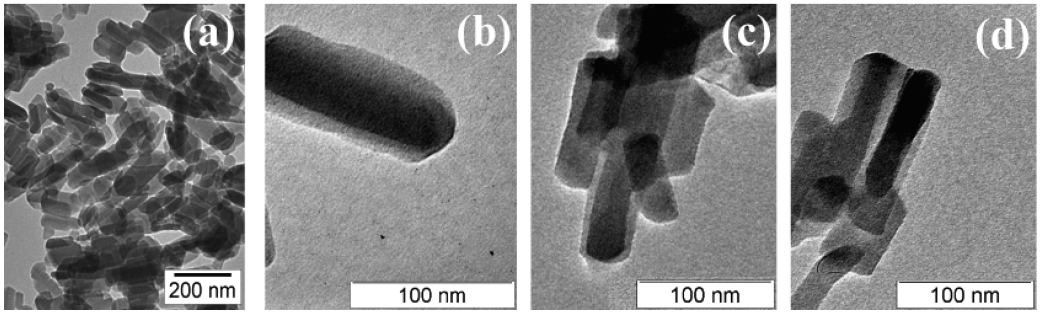

Figure 1. Transmission electron microscopy images of (a) unmodified gadolinium (Gd) metal−organic framework (MOF) nanoparticles, along with Gd MOF nanoparticles modified with (b) poly[*N*-(2-hydroxypropyl)methacrylamide] ($M_{n,experimental}$ = 19 370 g/mol), (c) poly(*N*-isopropylacrylamide) ($M_{n,experimental}$ = 17 846 g/mol), and (d) polystyrene ($M_{n,experimental}$ = 15 245 g/mol) homopolymers synthesized by reversible addition−fragmentation chain transfer polymerization.

gravimetric analysis (TGA) was achieved on a Seiko TG/DTA 220 instrument calibrated against an indium standard. Alumina pans were used, and samples were run with a helium gas sweep. The heating program was as follows: 30−110 °C at 20 °C/min, hold 30 min at 110 °C, heat from 110 to 850 at 7 °C/min, hold at 850 °C for 30 min, then cool to 30 °C. ICP AES data were acquired on a Perkin-Elmer Optima 3000 ICP-AES instrument following the EPA 200.7 standardized method. The instrument was calibrated with an internal scandium standard and recalibrated if there was greater than 20% drift from the 50 ppm concentration. Samples were diluted in a 1% nitric solution to give a total volume of 10 mL and run against an internal quality control gadolinium standard from High Purity Standards using a two point calibration.

Results and Discussion

Nanoparticles offer tremendous potential in the general area of nanomedicines; however, their modification to provide critical properties such as biocompatibility, biomolecular targeting, multimodal imaging, and treatment capabilities is of utmost importance. In order to accomplish this, it is first important to provide a method for the reproducible, well-defined, and stable surface modification of the nanoparticles. Modification of nanoparticle surfaces with well-defined polymers synthesized via RAFT polymerization techniques offers one of the most versatile routes to enhancing the properties of high surface area nanoparticle structures. To date, RAFT polymers have been employed in the modification of a range of surfaces including gold, silver, and CdSe nanoparticles by reducing the RAFT agent end group to a thiol moiety and employing the "grafting to" approach.[23−26] Nanoparticle structures, such as gold nanorods and Gd nanoparticles, have seen recent interest due to their potential application as biomedical imaging agents in dark field microscopy and MRI, respectively.[1−3,5−9,11,13,15,31−34] Recently, focus has intensified on the utilization of Gd nanoparticles as positive contrast agents for diagnostic imaging using MRI; however, despite a great deal of interest, there has been nominal research on the modification of Gd nanoparticles with well-defined polymers to provide increased functionality, such as biocompatibility and tunable imaging properties, for applications such as well-defined nanomedicines. As such, it is important to develop a surface modification technique that allows the attachment of well-defined, functional RAFT polymers and provides an understanding of the effects of polymer modification on their MRI relaxivity characteristics.

Synthesis of Gd MOF Nanoparticles. This research focused on the development of a novel surface modification technique for nanoscale Gd MOFs with well-defined polymers synthesized via RAFT polymerization techniques. The use of Gd MOF nanoparticles as positive contrast agents for MRI should provide several advantages over the clinically employed Gd chelates, such as enhanced imaging through magnetic resonance, increased biostability, and longer *in vivo* retention.[2,5−11,13,33] Gd-based contrast agents produce a large shortening of the longitudinal relaxation time (T1) and high longitudinal relaxivity (r_1) and are called positive contrast agents, where the relaxivity value, r, is simply defined as the inverse of the relaxation time with respect to the contrast agent concentration.[13,35] Conversely, negative contrast agents, such as SPIOs, typically induce a large shortening of the transverse relaxation time (T2) and a high transverse relaxivity (r_2), leading to a darkening effect.[13,35] The ratio of r_2/r_1 is used to provide information about the contrast agent, where r_2/r_1 values below 2 show brightening in T1-weighted images, providing a positive contrast agent.[13] Generally, there is a preference for the use of positive contrast agents based on Gd^{3+} at the clinical level due to their wider dynamic range. The Gd MOF nanoparticles used in this research were prepared via a reverse microemulsion procedure developed by Reiter and co-workers.[2] The Lin group has discussed the synthesis along with the chemical and physical properties of Gd MOF nanoparticles in detail in the literature.[2,3,36] The synthesis procedure for the Gd MOF nanoparticles employed a water to surfactant ratio of 10, 0.05 M $GdCl_3$ and 0.075 M 1,4-BDC, and the resultant nanoparticles were characterized using TEM (Figure 1) and ATR-FTIR (Figure 2), along with XRD and TGA (Supporting Information). The TEM image (Figure 1a) shows the synthesis of Gd MOF nanoparticles with an average length of 122 ± 30 nm and width of 53 ± 12 nm. The ATR-FTIR spectrum (Figure 2c) showed a characteristic out-of-plane =C−H aromatic stretch at 725 cm^{-1}, a symmetric carboxylate stretch at 1400 cm^{-1}, an asymmetric carboxylate stretch at 1540 cm^{-1}, along with 2855, 2925, and 3065 cm^{-1}, which are attributed to the −C−H stretching vibrations of the 1,4-BDC bridging ligand, and 3460 cm^{-1} which was attributed to the −OH stretch of the water ligand. The ATR-FTIR spectrum of the Gd MOF nanoparticles compared well with the spectrum of a similar nanoscale MOF synthesized with the 1,4-BDC ligand, which has been previously discussed

(31) Hartman, K. B.; Laus, S.; Bolskar, R. D.; Muthupillai, R.; Helm, L.; Toth, E.; Merbach, A. E.; Wilson, L. J. *Nano Lett.* **2008**, *8*, 415–419.
(32) Kim, J. S.; Rieter, W. J.; Taylor, K. M. L.; An, H.; Lin, W.; Lin, W. *J. Am. Chem. Soc.* **2007**, *129*, 8962–8963.
(33) Reynolds, C. H.; Annan, N.; Beshah, K.; Huber, J. H.; Shaber, S. H.; Lenkinski, R. E.; Wortman, J. A. *J. Am. Chem. Soc.* **2000**, *122*, 8940–8945.
(34) Allen, M.; Bulte, J. W. M.; Liepold, L.; Basu, G.; Zywicke, H. A.; Frank, J. A.; Young, M.; Douglas, T. *Magn. Reson. Med.* **2005**, *54*, 807–812.
(35) Caravan, P.; Ellison, J. J.; McMurry, T. J.; Lauffer, R. B. *Chem. Rev.* **1999**, *99*, 2293–2352.
(36) Lin, W.; Rieter, W. J.; Taylor, K. M. L. *Angew. Chem., Int. Ed.* **2009**, *48*, 650–658.

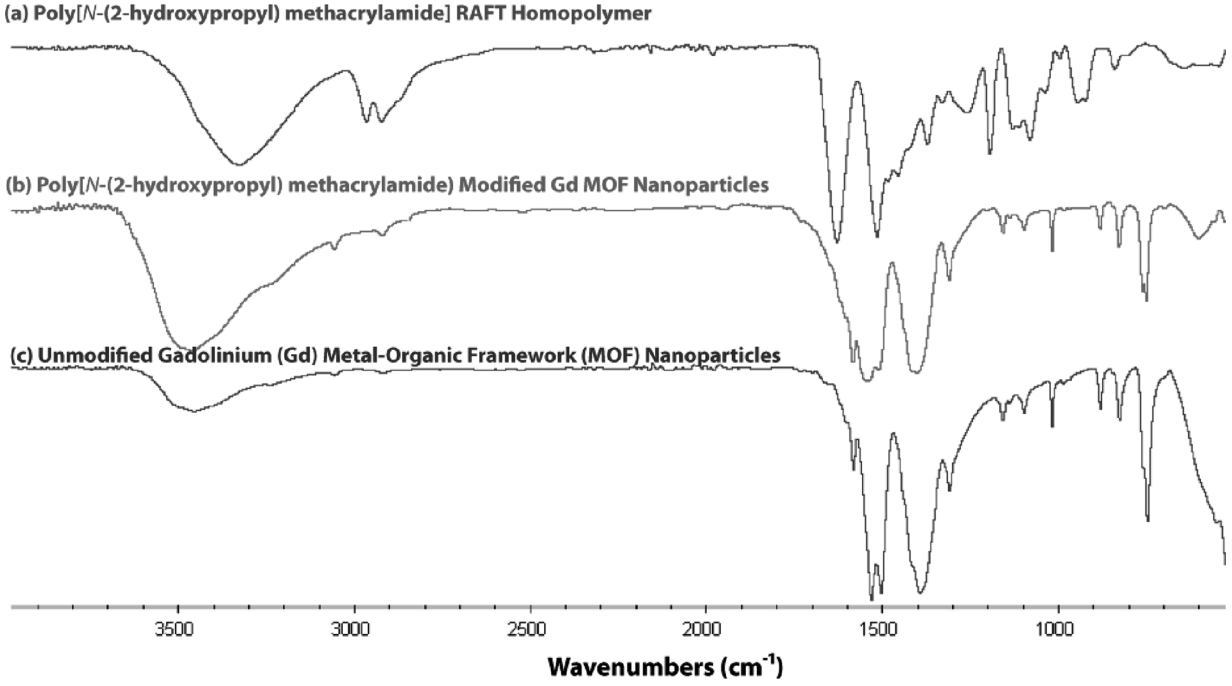

Figure 2. ATR-FTIR spectra of the (a) poly[*N*-(2-hydroxypropyl)methacrylamide] (PHPMA) homopolymer synthesized by reversible addition−fragmentation chain transfer polymerization, (b) PHPMA homopolymer modified gadolinium (Gd) metal−organic framework (MOF) nanoparticles, and (c) unmodified Gd MOF nanoparticles.

in the literature.[37] Additionally, TGA was employed and confirmed the empirical formula of the Gd MOF nanoparticles to be $Gd(1,4\text{-}BDC)_{1.5}(H_2O)_2$, as discussed in the literature.[2]

Synthesis and Characterization of RAFT Polymers. To demonstrate the versatility of the newly developed procedure to surface modify Gd MOF nanoparticles, PHPMA, PSty, PNIPAM, PDMAEA, PPEGMEA, and PAA homopolymers were each synthesized via RAFT polymerization techniques employing the RAFT agent, DATC, for subsequent deposition onto the Gd MOF nanoparticles. Each of these polymers, except PSty, were chosen because of their utility as polymers for biobased applications and positive results toward biocompatibility.[38−41] PSty was chosen both to demonstrate the inherent flexibility of the surface modification procedure, by using a hydrophobic polymer, and to determine the effect of a hydrophobic coating on the relaxation properties of the Gd MOF nanoparticles. By taking advantage of the living and well-defined nature of RAFT polymerization, the molecular weight of the polymers can be easily controlled by simply varying the ratio of monomer to RAFT agent and the extent of conversion of the polymerization. Table 1 shows experimental and theoretical molecular weights for each of the homopolymers synthesized by RAFT polymerization. As can been seen in Table 1, each of the polymerizations showed good agreement between the theoretical and experimental molecular weights. For example, the experimental molecular weight of PHPMA of 19 696 g/mol corresponded well to the theoretical molecular weight of 19 370 g/mol (Table 1). In conjunction to molecular weight control, well-defined RAFT polymerizations typically provide polymers with narrow molecular weight distributions. Table 1 demonstrates that the polydispersity index (PDI) for each of the copolymers synthesized was generally low and each GPC curve indicated monomodal molecular weight distributions. The good agreement between experimental and theoretical molecular weights and the narrow molecular weight distributions obtained for each of the homopolymers indicates in each case a well-defined RAFT polymerization was achieved and that virtually all polymer chains prepared should contain a trithiocarbonate end group, due to the living nature of the polymerization, which can be used to attach the RAFT polymers to the Gd MOF nanoparticles.

Surface Modification of Gd MOF Nanoparticles with RAFT Homopolymers. The limitations inherent with current nanoparticle systems, such as aggregation, *in vivo* toxicity, and poor biostability, have led to a great deal of interest in surface modification with well-defined polymers as a means of incorporating advanced functionality and biocompatibility into nanomedical devices.[10,42−45] As discussed previously, the modification of Gd nanoparticles has been focused on either the encapsulation in an emulsifying wax or functionalization of the surface with inorganic materials, such as a silica shell.[3,5−9,15,32] As such, the development of a surface modification technique for nanoscale Gd MOFs with well-defined polymers synthesized via RAFT polymerization offers great potential for the formation of novel nanomedicines. As mentioned above, due to the living nature of RAFT polymerizations and a low amount of termination during the polymerization, RAFT polymers contain a high degree of chain end functionality, which imparts chain ends with a thiocarbonylthio moiety.[46] As DATC is employed as the RAFT agent

(37) Reineke, T. M. E. M.; Fehr, M.; Kelley, D.; Yaghi, O. M. *J. Am. Chem. Soc.* **1999**, *121*, 1651–1657.
(38) Vihola, H.; Laukkanen, A.; Valtola, L.; Tenhu, H.; Hirvonen, J. *Biomaterials* **2005**, *26*, 3055–3064.
(39) Lee, K. Y.; Yuk, S. H. *Prog. Polym. Sci.* **2007**, *32*, 669–697.
(40) You, Y.-Z.; Manickam, D. S.; Zhou, Q. H.; Oupický, D. *J. Controlled Release* **2007**, *122*, 217–225.
(41) Tugulu, S.; Klok, H.-A. *Biomacromolecules* **2008**, *9*, 906–912.
(42) Strijkers, G. J.; Mulder, W. J. M.; van Tilborg, G. A. F.; Nicolay, K. *Anti-Cancer Agents Med. Chem.* **2007**, *7*, 291–305.
(43) LaConte, L.; Nitin, N.; Bao, G. *Mater. Today* **2005**, *8*, 32–38.
(44) Taylor, K. M. L.; Jin, A.; Lin, W. *Angew. Chem., Int. Ed.* **2008**, *47*, 7722–7725.
(45) van Schooneveld, M. M.; Vucic, E.; Koole, R.; Zhou, Y.; Stocks, J.; Cormode, D. P.; Tang, C. Y.; Gordon, R. E.; Nicolay, K.; Meijerink, A.; Fayad, Z. A.; Mulder, W. J. M. *Nano Lett.* **2008**, *8*, 2517–2525.
(46) Perrier, S.; Takolpuckdee, P. *J. Polym. Sci., Part A: Polym. Chem.* **2005**, *43*, 5347–5393.

Table 1. Comparison of Molecular Weight Properties of RAFT Homopolymers with Polymer Coating Thickness and Grafting Density

	M_n (g/mol)				grafting density (chain/nm^2)	
polymer coating	theory[a]	experimental[b]	PDI[b,e]	coating thickness (nm)[f]	theory[g]	experimental[h,i]
PHPMA	5129	5300	1.44	2.4 ± 1.1	0.1847	0.1379
	9073	10 200	1.30	3.5 ± 0.7	0.0957	0.0993
	19 696	19 400	1.24	7.3 ± 0.6	0.0729	0.0638
PNIPAM	5500	5700	1.23	4.2 ± 0.3	0.1849	0.1395
	8733	8600	1.12	7.0 ± 0.4	0.1591	0.1037
	17 109	17 800	1.12	10.9 ± 1.0	0.1070	0.0873
PSty	4938	4800	1.15	1.6 ± 0.3	0.1660	0.1839
	9378	9000	1.15	5.7 ± 0.9	0.1341	0.0960
	18 928	15 300	1.13	8.7 ± 0.9	0.1033	0.0815
PDMAEA	17 451	15 100	1.25	5.1 ± 0.3	0.1276	0.1111
PPEGMEA	25 920	19 600	1.29	4.4 ± 1.0	0.0792	0.0636
PAA	14 335	10 800[c]		5.7 ± 0.7	0.1545	0.1147
		10 900[d]	1.10[d]		1.1538	0.1142

[a] $M_{n,\ theoretical}$ for each RAFT polymerization was calculated using the equation M_n = (molecular weight of RAFT agent) + (molecular weight of monomer) × ([monomer]$_0$/[RAFT agent]$_0$) × (monomer conversion). [b] Determined by gel permeation chromatography. [c] Calculated by end-group analysis using ^{1}H NMR. [d] Determined by matrix assisted laser desorption ionization-time-of-flight mass spectrometry. [e] Polydispersity index (PDI) was calculated using the equation PDI = (M_w/M_n). [f] Polymer coating thickness was determined by transmission electron microscopy, and is an average of 10 measurements. [g] Theoretical grafting densities were calculated from equations discussed in the literature using an average Gd MOF nanoparticle length of 122 nm and width of 53 nm, along with the experimental molecular weight and bulk density of each polymer. [h] Experimental grafting densities were calculated using an average Gd MOF nanoparticle length of 122 nm and width of 53 nm, the experimental molecular weight of each polymer, a bulk density of 2.529 g/cm^3 for the Gd MOF nanoparticles, along with the mass of polymer per mass of Gd MOF nanoparticle determined by thermogravimetric analysis. [i] Percent relative standard deviations were determined to be <7% for the experimental grafting density calculations.

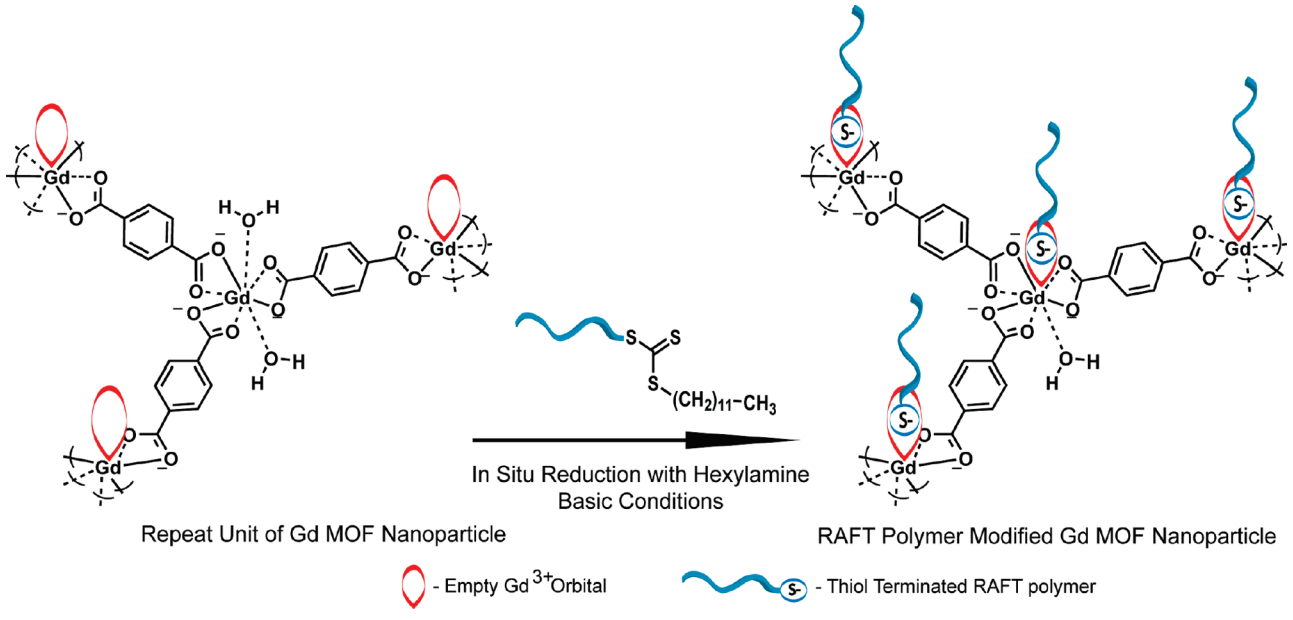

Figure 3. Proposed "grafting to" technique for coordination of thiolate polymer chain ends to gadolinium (Gd) metal−organic framework (MOF) nanoparticles synthesized by a reverse microemulsion system employing the 1,4-benzenedicarboxylic acid ligand.

in the formation of homopolymers by RAFT polymerization in this study, all of the homopolymers produced should have trithiocarbonate terminated chains. The surface modification of the Gd MOF nanoparticles was achieved by the "grafting to" technique, which involved an initial aminolysis, using hexylamine, of the trithiocarbonate end group of the RAFT homopolymers to a thiolate functionality under inert and basic conditions. Subsequently, it is hypothesized that the thiolate terminated homopolymer was covalently attached to the nanoparticle surface through a coordination reaction between the thiolate end group moiety and vacant orbitals on the Gd^{3+} ions at the surface of the Gd MOF nanoparticles (Figure 3). Attachment of the polymer chain to the surface of the Gd MOF nanoparticles via coordination of the thiolate end group has been proposed, as thiols are known to form stable metal thiolate compounds with many metal ions under basic conditions, and thiolates are also known to

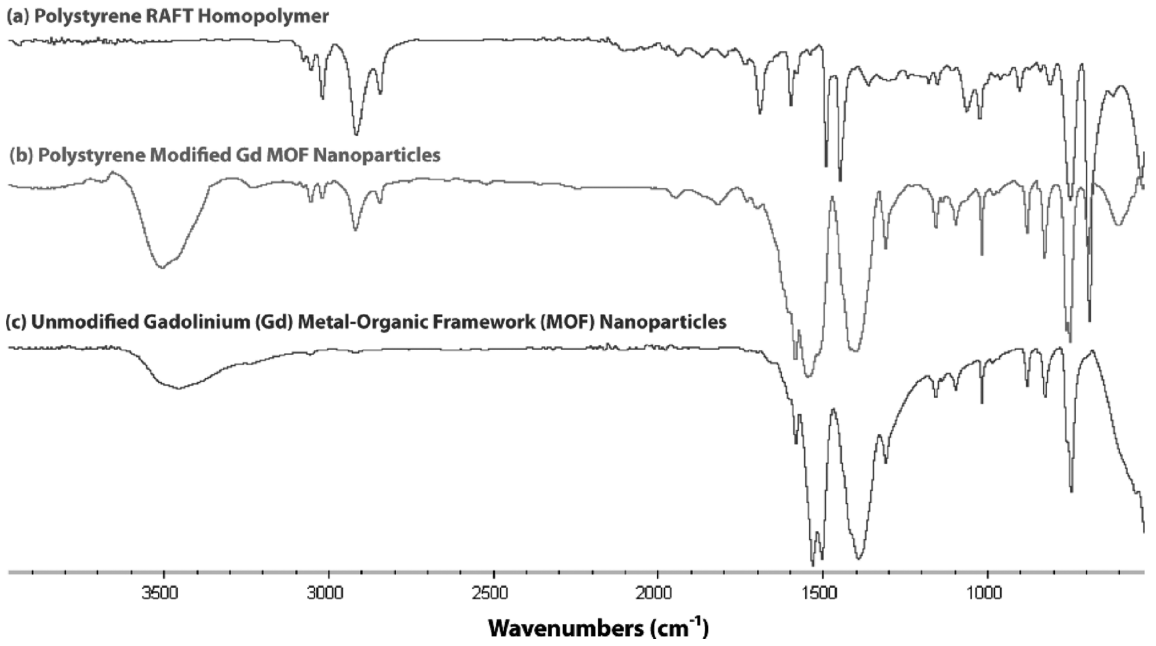

Figure 4. ATR-FTIR spectra of the (a) polystyrene (PSty) homopolymer synthesized by reversible addition−fragmentation chain transfer polymerization, (b) PSty homopolymer modified gadolinium (Gd) metal−organic framework (MOF) nanoparticles, and (c) unmodified Gd MOF nanoparticles.

coordinate strongly to many organometallic compounds including iron porphyrins.[47,48] Further evidence for and discussion of the attachment mechanism for the RAFT polymers to the surface of the Gd MOF nanoparticles is included at the end of this section. Using this procedure, Gd MOF nanoparticles were modified with the various RAFT homopolymers prepared in the previous section. It should be noted that, after polymer deposition and prior to characterization or use, the nanoparticles were washed several times with a good solvent for the polymer, via repeated washing and centrifugation steps, to remove any untethered polymer from the system.

Prior to attachment of the RAFT polymers to the Gd MOF nanoparticles, ^{1}H NMR, UV−vis spectroscopy, and ATR-FTIR were used to verify the conversion of the trithiocarbonate end group to a thiolate upon addition of the hexylamine (results not shown). In each case, the aminolysis reaction resulted in approximately quantitative conversion of the RAFT polymer end groups to thiolates, as had been observed in the literature for similar reactions,[23,49,50] with minimal dimerization confirmed by ^{1}H NMR and GPC. Surface modification of the Gd MOF nanoparticles with RAFT homopolymers was characterized through both TEM (Figure 1b−d, Table 1, and Supporting Information) and ATR-FTIR spectroscopy (Figures 2 and 4, and Supporting Information). The Gd MOF nanoparticles were first modified with PHPMA homopolymer synthesized via RAFT polymerization, and ATR-FTIR was utilized to confirm the addition of the PHPMA homopolymer onto the surface of the nanoparticles (Figure 2). Three PHPMA samples of different molecular weight, 5327, 10 281, and 19 370 g/mol, were used to modify the Gd MOF nanoparticles. The different PHPMA samples were used to examine the effect of molecular weight on grafting density, coating thickness, and relaxivity. Upon modification of the Gd MOF nanoparticles, several of the characteristic stretches of the free PHPMA homopolymer, including a combined broad N−H and O−H stretch above 3300 cm^{-1} and a small N−H bend at 1640 cm^{-1} indicating the presence of the acrylamide functionality, an increase in intensity of the $-CH_2$ stretching and C−H stretching vibrations between 2900 and 3100 cm^{-1} due to backbone methylenes, a peak at 1720 cm^{-1} assigned to the carbonyl stretch of the amide, and broadening of the stretch at 1490 cm^{-1} attributed to the −NH− group, display good transference to the polymer modified Gd MOF nanoparticles, when compared to the unmodified Gd MOF nanoparticles (Figure 2). It should be noted that the relative increase in intensity of these peaks is small due to the small coating thickness in comparison to the size of the Gd MOF nanoparticle. TEM was employed to determine the thickness of the PHPMA on the surface of the Gd MOF nanoparticles. The TEM images (Figure 1b and Supporting Information) indicate a uniform coating for each of the PHPMA homopolymers on the surface of the Gd MOF nanoparticles after deposition. There was also a trend of increasing polymer coating thickness with molecular weight of the polymer. For example, the average thickness of the PHPMA homopolymer with $M_{n,experimental}$ of 5327 g/mol is approximately 2.4 ± 1.1 nm (Table 1). The PHPMA homopolymer with $M_{n,experimental}$ equal to 10 281 g/mol increased the polymer coating thickness to 3.5 ± 0.7 nm, while that with $M_{n,experimental}$ of 19370 g/mol further raised the thickness to 7.3 ± 0.6 nm (Table 1). This trend suggests the ability to tailor the polymer coating thickness by simply changing the molecular weight characteristics of the RAFT polymer used for modification.

The Gd MOF nanoparticles were next modified with a series of different molecular weight PNIPAM homopolymers synthesized via RAFT polymerization. ATR-FTIR was employed to confirm the addition of the PNIPAM homopolymer onto the surface of the Gd MOF nanoparticles. Several of the characteristic stretches of the free PNIPAM homopolymer, including a broad N−H stretch above 3300 cm^{-1} and a small N−H bend at 1640 cm^{-1} indicating the presence of the acrylamide functionality, an

(47) Larsen, T. H.; Sigman, M.; Ghezelbash, A.; Doty, R. C.; Korgel, B. A. *J. Am. Chem. Soc.* **2003**, *125*, 5638–5639.
(48) Urano, Y.; Higuchi, T.; Hirobe, M.; Nagano, T. *J. Am. Chem. Soc.* **1997**, *119*, 12008–12009.
(49) Xu, J.; He, J.; Fan, D.; Wang, X.; Yang, Y. *Macromolecules* **2006**, *39*, 8616–8624.
(50) Moad, G.; Chong, Y. K.; Postma, A.; Rizzardo, E.; Thang, S. H. *Polymer* **2005**, *46*, 8458–8468.

increase in intensity of the $-CH_2$ stretching and C−H stretching vibrations between 2800 and 3000 cm^{-1} due to backbone methylenes, a peak at 1720 cm^{-1} assigned to the carbonyl stretch of the amide, and a stretch at 1380 cm^{-1} attributed to the addition of $-CH_3$ and isopropyl groups, display good transference to the polymer modified Gd MOF nanoparticles, when compared to the unmodified Gd MOF nanoparticles (Supporting Information). The TEM images (Figure 1c and Supporting Information) show a relatively uniform coating of the PNIPAM homopolymers around the Gd MOF nanoparticles after deposition. As was seen above, there is a definite trend of increasing polymer coating thickness with molecular weight of the polymer (Table 1). For example, the average thickness of the PNIPAM homopolymer with $M_{n,experimental}$ of 5690 g/mol is approximately 4.2 ± 0.3 nm (Table 1). The PNIPAM homopolymer with $M_{n,experimental}$ equal to 8606 g/mol increased the polymer coating thickness to 7.0 ± 0.4 nm, while that with $M_{n,experimental}$ of 17 846 g/mol further raised the thickness to 10.9 ± 1.0 nm (Table 1).

Three different molecular weight PSty homopolymers synthesized via RAFT polymerization were next employed to surface modify the Gd MOF nanoparticles. As mentioned above, the use of PSty should result in a more hydrophobic coating on the Gd MOF nanostructure and may dramatically affect the relaxation properties of the particles. The presence of PSty on the Gd MOF nanoparticles was confirmed due to the good transference of aromatic C−H stretching around 3100 cm^{-1} and C=C aromatic doublets at 1420−1480 cm^{-1} from the free polymer to the polymer modified Gd MOF nanoparticles, when compared to the unmodified Gd MOF nanoparticles (Figure 4). As discussed above, the TEM images (Figure 1d and Supporting Information) of the PSty modification of Gd MOF nanoparticles showed a similar trend with respect to increasing polymer molecular weight and increasing coating thickness. The average thickness of the PSty homopolymer with $M_{n,experimental}$ of 4802 g/mol is approximately 1.6 ± 0.3 nm (Table 1). The PSty homopolymer with $M_{n,experimental}$ equal to 8972 g/mol increased the polymer coating thickness to 6.7 ± 0.9 nm, while that with $M_{n,experimental}$ of 15 245 g/mol further raised the thickness to 8.7 ± 0.9 nm (Table 1). In addition to the molecular weight of the PSty tuning the polymer thickness characteristics, the PSty modified Gd MOF nanoparticles showed a decreased solubility in aqueous solution with increasing molecular weight. This trend was attributed to the successful modification of the Gd MOF nanoparticles with the highly hydrophobic PSty polymer.

Next, PDMAEA homopolymer with a molecular weight of 15 120 g/mol was deposited onto the Gd MOF nanoparticles after reduction of the trithiocarbonate end groups under basic conditions to thiolates. Only one molecular weight of PDMAEA was used in this study. The TEM image showed a fairly uniform coating of polymer around the Gd MOF nanoparticles after deposition, with an average thickness of approximately 5.1 ± 0.3 nm (Table 1 and Supporting Information). The ATR-FTIR spectrum (Supporting Information) showed good transference of the methylene vibrations between 2700 and 2850 cm^{-1}, the carbonyl stretch of the ester at 1705 cm^{-1}, the stretching vibrations near 2810 cm^{-1} attributed to the $-CH_3$, and 1150 cm^{-1} correlated to the C−N of $-N(CH_3)_2$ of the PDMAEA homopolymer to the polymer modified Gd MOF nanoparticles.

The Gd MOF nanoparticles were also modified with the PPEGMEA homopolymer synthesized via RAFT polymerization; once again only one molecular weight of PPEGMEA was used in this study. ATR-FTIR spectra (Supporting Information) showed good transference of the inherent peaks of the PPEGMEA homopolymer to the modified Gd MOF nanoparticles including a broad stretch between 3055 and 2650 cm^{-1} characteristic of C−H stretching vibrations of backbone and side chain $-CH_2$ and $-CH_3$, 1730 cm^{-1} attributed to the C=O stretching vibration of the ester, and asymmetric and symmetric C−O stretching vibrations at 1100 cm^{-1} and 950 cm^{-1} characteristic of the aliphatic ester. TEM images showed that PPEGMEA with a molecular weight of 19 542 g/mol produced a coating with an average thickness of 5.2 ± 1.3 nm on the Gd MOF nanoparticles (Table 1 and Supporting Information).

Finally, the Gd MOF nanoparticles were surface modified with a PAA homopolymer with a molecular weight of 10 888 g/mol synthesized via RAFT polymerization. TEM and ATR-FTIR were employed to confirm the surface modification of the Gd MOF nanoparticles with PAA homopolymer. TEM images provided evidence of a PAA coating around the Gd MOF nanoparticles of 5.7 ± 0.7 nm (Table 1 and Supporting Information). ATR-FTIR spectra (Supporting Information) showed good transference of the inherent peaks of the PAA homopolymer to the modified Gd MOF nanoparticles including a broad stretch between 3000 and 3600 cm^{-1} attributed to −OH stretching of the carboxylic acid, along with broadening of the carbonyl stretch vibrations due to overlap of the carboxylic acid and unprotonated carboxylate functionalities between 1500 and 1700 cm^{-1}.

The above results have demonstrated, by employing a wide range of well-defined polymers of different functionality, that the proposed novel surface modification technique for Gd MOF nanoparticles using RAFT polymers provides well-defined polymer modified nanoparticles, along with the ability to tune both the polymer coating thickness and potentially the relaxation properties. However, the stability of the polymer modified positive contrast nanoparticle agents produced in this work is of critical importance, as recently there has been an increasing focus on nephrogenic fibrosing dermopathy.[51−53] Though our group has recently published results that demonstrate the polymer modified Gd MOF nanoparticles show improved stability, with respect to loss of Gd^{3+}, it is also important to discuss the stability of the polymer coating itself. Experimental results have shown that RAFT polymer coating stability is quite robust. TEM and ATR-FTIR have confirmed the persistence of the RAFT polymer coatings on the Gd MOF nanoparticles after being stored in aqueous and organic medium over several months. Furthermore, solutions of polymer modified Gd MOF nanoparticles have been heated near physiological temperatures, which confirmed the continued integrity of the polymer surface modification. These results have further demonstrated that the polymers used to surface modify the Gd MOF nanoparticles demonstrate excellent stability over long periods of time and at physiological temperatures.

As discussed in the beginning of this section, we have hypothesized that attachment of the RAFT polymers to the surface of the Gd MOF nanoparticles is via coordination of the thiolate end group of the polymer with vacant orbitals on the Gd^{3+} ions at the surface of the nanoparticles (Figure 3). In an attempt to confirm this hypothesis, the attachment of the RAFT polymer to the surface of the Gd MOF nanoparticles was investigated without the addition of hexylamine. This involved conducting exactly the same procedure described above for attachment of PNIPAM prepared by RAFT polymerization, except no hexylamine was added to the system. TEM was employed to monitor modification of the Gd MOF nanoparticles and confirmed that the attachment

(51) Cowper, S. E. *Am. J. Kidney Dis.* **2005**, *46*, 763–765.
(52) Grobner, T. *Nephrol., Dial., Transplant.* **2006**, *21*, 1104–1108.
(53) High, W. A.; Ayers, R. A.; Chandler, J.; Zito, G.; Cowper, S. E. *J. Am. Acad. Dermatol.* **2007**, *56*, 21–26.

of the trithiocarbonate end-functional PNIPAM RAFT homopolymer was unsuccessful, as no polymer coating was visible in the microscopy images (Supporting Information). ATR-FTIR spectroscopy also demonstrated that the modification of Gd MOF nanoparticles without the addition of a reducing agent was unsuccessful, as there were nominal changes between the unmodified and modified Gd MOF nanoparticles (Supporting Information). Without the addition of a nucleophile to form thiolate polymer end groups, Gd MOF nanoparticles were not successfully modified. This was attributed to the inability of the trithiocarbonate polymer end group to coordinate itself with the empty orbitals of the Gd^{3+} of the Gd-based nanoscale MOF. This confirmed that the thiolate end groups of the RAFT polymer, formed after aminolysis, were critical for attachment of the polymers and suggested that the thiolate end groups were coordinating to empty orbitals of the Gd^{3+} of the Gd NP surface, as hypothesized in Figure 3.[47,48]

To provide further evidence that the thiolate moiety was indeed allowing attachment of the RAFT homopolymers to the surface of the Gd MOF nanoparticles, a small molecule model, dodecanethiol, was employed to modify the surface of the Gd MOF nanoparticles under basic conditions. The ATR-FTIR spectra for the modification of Gd MOF nanoparticles with dodecanthiolate showed an increase in intensity of the C−H stretching attributed to the $-CH_2$ and $-CH_3$ moieties (Supporting Information). Due to the small size of the dodecanethiol molecule, TEM images did not show changes to the surface of the Gd MOF nanoparticles after modification. However, similar to the hydrophobic PSty modified Gd MOF nanoparticles, the dodecanthiolate modified Gd MOF nanoparticles showed a high degree of insolubility in water. This was attributed to the incorporation of a hydrophobic dodecyl group attached to the Gd MOF nanoparticles. These results confirmed the successful modification of the Gd MOF nanoparticles and substantiated the hypothesis that the thiolate of the dodecanethiol provided an attachment point to the Gd MOF nanoparticles through an analogous route, as described in Figure 3, to the polymer modification.

Calculation of Polymer Grafting Density per Gd MOF Nanoparticle. The development or application of any surface modification technique using polymers requires knowledge of critical elements such as the mode of modification, evidence of the polymer on the surface, and the stability of the polymer coating, all of which have been discussed above. Another element which is critical in all surface modification techniques is an understanding of the amount of polymer attached to the surface, as this has a vital role in determining the conformation of the polymer on the surface. As such, the grafting density (σ), defined as number of chains tethered per unit area, was calculated utilizing both theoretical and experimental equations from the literature (Supporting Information).[54−60] First, the average volume and surface area of a Gd MOF nanoparticle was determined assuming a rodlike shape based on the average length of 122 nm and width of 53 nm, which were determined from TEM images (Figure 1 and Supporting Information). Second, the experimental number average molecular weight of each polymer sample (Table 1) was employed for both the experimental and theoretical grafting calculations. Next, the bulk density of the Gd MOF nanoparticles was determined by XRD (Supporting Information) to be approximately 2.529 g/cm^3, which compared well to literature values.[2,44] Finally, the bulk density of each polymer was determined from literature values.[54,61−63] Table 1 shows both the theoretical and experimental grafting density values for each of the polymer modified Gd MOF nanoparticle samples calculated from the equations shown in the Supporting Information. As can be seen in Table 1, the theoretical and experimental grafting densities for each of the polymers used for surface modification of the Gd MOF nanoparticles correlated quite well, with nearly all of the experimental calculations being within 25% of their theoretical grafting densities. For example, the PHPMA homopolymer with a molecular weight of 5327 g/mol was employed to modify Gd MOF nanoparticles providing comparable theoretical and experimental polymer grafting densities of 0.1847 and 0.1379 chain/nm^2, respectively. In each case, the grafting densities are relatively high for use of a "grafting to" technique, as most of the samples have values around 0.1 chains/nm^2, providing modification of the Gd MOF nanoparticles with each polymer in the "brush" regime.[57,59,64] However, though the values obtained are quite high, similar experimental grafting densities have been documented in the literature for the "grafting to" technique.[56,65−67] Despite the high grafting density values, a definite trend was seen, which showed a decrease in the grafting density with increased molecular weight of the grafted polymer (Table 1). For example, as the molecular weight of the PHPMA increased from 5327 to 10 281 g/mol, the experimental grafting density decreased from 0.1379 to 0.0993 chains/nm^2. The experimental grafting density further decreased to 0.0638 chains/nm^2 with modification of the Gd MOF nanoparticles using the PHPMA homopolymer with an experimental molecular weight of 19 370 g/mol. This trend of decreasing grafting density with increasing polymer molecular weight has been discussed extensively in the literature with the "grafting to" technique and is a result of limited diffusion of polymer chains to reactive sites on the nanoparticle surface due to increased steric hindrance of polymer chains that are already attached to the surface.[57,59,64] As such, as the molecular weight of the chains increases, it becomes more difficult for chains to diffuse to the surface, providing lower polymer grafting densities.

***In Vitro* MRI of Gd MOF Nanoparticles and Polymer Modified Gd MOF Nanoparticles.** MRI has become one of the most important and widely used techniques in medical diagnostics. An MR image is generated from the nuclear magnetic resonance of water protons, with the observed contrast in MRI essentially dependent on factors such as water proton density and the T1 and T2 values of these protons. Typically, contrast agents are used in MRI to aid in diagnostic imaging by increasing the contrast between the particular organ or tissue of interest and the surrounding tissues in the body. Historically Gd−chelate compounds have been used as positive contrast agents, as they

(54) Matsuda, Y.; Kobayashi, M.; Annaka, M.; Ishihara, K.; Takahara, A. *Langmuir* **2008**, *24*, 8772–8778.
(55) Roth, P. J.; Theato, P. *Chem. Mater.* **2008**, *20*, 1614–1621.
(56) Liu, Y.; Klep, V.; Zdyrko, B.; Luzinov, I. *Langmuir* **2004**, *20*, 6710–6718.
(57) Advincula, R. C.; Brittain, W. J.; Caster, K. C.; Ruhe, J. *Polymer Brushes: Synthesis, Characterization, Applications*; Wiley-VCH Verlag GmbH & Co.: Weinheim, 2004.
(58) Halperin, A.; Tirrell, M.; Lodge, T. P. *Adv. Polym. Sci.* **1992**, *100*, 31–71.
(59) Jordan, R., Ed. *Surface initiated polymerization I and II: Advances in polymer science*; Springer: Berlin, Heidelberg, New York, 2006.
(60) Sevick, E. M. *Macromolecules* **1996**, *29*, 6952–6958.
(61) Dong, H.; Matyjaszewski, K. *Macromolecules* **2008**, *41*, 6868–6870.
(62) Miller, R. L. *Polymer Handbook*, 4th ed.; John Wiley & Sons: New York, 1999.
(63) Furuta, I.; Kimura, S.-I.; Iwama, M. *Polymer Handbook*, 4th ed.; John Wiley & Sons: New York, 1999.
(64) Boyes, S. G.; Granville, A. M.; Baum, M.; Akgun, B.; Mirous, B. K.; Brittain, W. J. *Surf. Sci.* **2004**, *570*, 1–12.
(65) Motornov, M.; Sheparovych, R.; Katz, E.; Minko, S. *ACS Nano* **2008**, *2*, 41–52.
(66) Muthukrishnan, S.; Erhard, D. P.; Mori, H.; Muller, A. H. E. *Macromolecules* **2006**, *39*, 2743–2750.
(67) Gao, H.; Matyjaszewski, K. *J. Am. Chem. Soc.* **2007**, *129*, 6633–6639.

produce a large shortening of T1 relaxation times and high longitudinal relaxivity (r_1), which has become one of the most effective mechanisms to brighten T1-weighted images.[13,35] Relaxivity values, r_1, and transverse relaxivity, r_2, are defined as the inverse of the measured T1 and T2 relaxation values, respectively, in relation to the concentration of Gd^{3+} in the contrast agent. The ratio of r_2/r_1 is used to provide information about the contrast agent, where values between 1 and 2 provide brightening in T1-weighted images, and are employed as positive contrast agents.[13] Although clinically employed MRI contrast agents, such as gadopentetate dimeglumine (Magnevist) and gadobenate dimeglumine (Multihance), are widely used, recent literature has shown that Gd^{3+} containing nanoscale MOFs could offer specific advantages as positive contrast agents for MRI due to their enhanced relaxivities and improved retention times.[2,10,11,13,15,31−33] However, as discussed above, application of Gd nanoparticles has been limited due to the difficulty in producing nanoparticles which are biocompatible, stable, and have specific surface functionality. While researchers have attempted to use surface modification techniques to overcome these limitations, success has been very limited. The surface modification technique presented above potentially provides a method to overcome all of these limitations. To further validate this method and its potential clinical use, it is important to examine the effect of polymer modification and functionality on the MRI properties of these structures.

In order to provide information about the clinical imaging viability of the polymer modified Gd MOF nanoparticles, as positive contrast nanoparticle agents, *in vitro* MRI was employed to determine relaxation properties of the unmodified and polymer modified Gd MOF nanoparticles. Table 2 compares the relaxivity values collected on a 1.5 T scanner for unmodified Gd MOF nanoparticles, each of the polymer modified Gd MOF nanoparticles, and the clinically employed contrasts agents, Magnevist and Multihance. The associated relaxivity curves for each of the Gd MOF nanoparticle samples, which compare their relaxation rates with respect to Gd^{3+} concentration against the clinically employed contrast agents, are shown in the Supporting Information. The longitudinal relaxivity values demonstrate that both the unmodified and polymer modified Gd MOF nanoparticles result in a large shortening of the T1 relaxation time and, thus, behave as positive contrast agents (Table 2). Of particular note is the fact that the polymer modification of the Gd MOF nanoparticles with the PHPMA, PNIPAM, PDMAEA, PPEGMEA, and PAA RAFT homopolymers demonstrated significantly higher relaxivity values in comparison to both the unmodified Gd MOF nanoparticles and the clinically employed small molecule contrast agents (Table 2). This phenomenon is attributed to increased water retention by the hydrophilic RAFT homopolymer matrices attached to the surface of the Gd MOF nanoparticles. The increased water retention allows for more favorable interactions between the water protons and the free orbitals of the Gd^{3+} containing MOF nanoparticle, thus enhancing T1 relaxation shortening effects. For example, when the highly hydrophilic PHPMA homopolymer, with a molecular weight of 19 370 g/mol, was employed for the modification of the Gd MOF nanoparticles, r_1 and r_2 values of 105.36 and 129.63 s^{-1} mM^{-1}, respectively, were determined (Table 2). These values are nearly 10 times higher than the observed relaxivities of the unmodified Gd MOF nanoparticles and 6 times higher than the values for the clinically employed Magnevist and Multihance (Table 2). Furthermore, in each case, the polymer modification of the Gd MOF nanoparticles provided a much lower r_2/r_1 value in comparison to both the unmodified Gd MOF nanoparticles and the clinically employed contrast agents (Table 2), which is advantageous for their use as clinical positive contrast agents. The other hydrophilic polymers, PNIPAM, PDMAEA, PPEGMEA, and PAA, showed similar drastically improved T1 shortening effects and lower r_2/r_1 values in comparison to both the unmodified Gd MOF nanoparticles and the clinical contrast agents (Table 2).

Next, in order to further establish the effect of chemical structure of the polymer on the relaxivity of the surface modified Gd MOF nanoparticles, the Gd MOF nanoparticles were surface modified with a highly hydrophobic polymer, PSty. The PSty modified Gd MOF nanoparticles showed very low longitudinal relaxivity values and very large transverse relaxivity values, which provided relaxivity ratio values more than 1 order of magnitude higher than the other polymer modified samples (Table 2).

Table 2. Experimental Relaxivity Data for Clinical Magnetic Resonance Imaging Contrast Agents, Multihance and Magnevist, along with the Unmodified and Polymer Modified Gadolinium Metal−Organic Framework Nanoparticles

contrast agent[a]	r_1 (s^{-1} mM^{-1})[b]	r_2 (s^{-1} mM^{-1})[b]	r_2/r_1
Magnevist	13.44	21.40	1.59
Multihance	19.45	30.44	1.57
unmodified Gd MOF nanoparticles	9.86	17.94	1.82
PHPMA (5327 g/mol) modified Gd MOF nanoparticles	17.81	25.77	1.45
PHPMA (10 281 g/mol) modified Gd MOF nanoparticles	32.94	44.85	1.36
PHPMA (19 370 g/mol) modified Gd MOF nanoparticles	105.36	129.63	1.23
PNIPAM (5690 g/mol) modified Gd MOF nanoparticles	20.27	29.73	1.47
PNIPAM (8606 g/mol) modified Gd MOF nanoparticles	46.99	64.10	1.36
PNIPAM (17 846 g/mol) modified Gd MOF nanoparticles	62.51	79.90	1.28
PSty (4802 g/mol) modified Gd MOF nanoparticles	1.17	14.16	12.10
PSty (8972 g/mol) modified Gd MOF nanoparticles	1.20	25.75	21.46
PSty (15 245 g/mol) modified Gd MOF nanoparticles	3.91	123.40	31.56
PDMAEA (15 120 g/mol) modified Gd MOF nanoparticles	37.20	54.17	1.46
PPEGMEA (19 542 g/mol) modified Gd MOF nanoparticles	59.93	81.55	1.36
PAA (10 888 g/mol) modified Gd MOF nanoparticles	21.30	31.82	1.49

[a] PHPMA = poly[*N*-(2-hydroxypropyl) methacrylamide], PNIPAM = poly(*N*-isopropylacrylamide), PSty = polystyrene, PDMAEA = poly-(2-(dimethylamino) ethyl acrylate), PPEGMEA = poly(((poly)ethylene glycol methyl ether) acrylate), and PAA = poly(acrylic acid). [b] Longitudinal relaxivity (r_1) and transverse relaxivity (r_2) values, calculated as the reciprocal values of the longitudinal relaxation time (T1) and transverse relaxation time (T2), respectively, of each of the contrast agents were determined with a 1.5 T scanner with samples diluted in deionized ultrafiltered water by acquiring signal intensity (I) measurements via region-of-interest analysis of the samples for all pulse sequences with T1 and T2 values being calculated using: $I_i = I_{o,i}(1 - \exp^{(-t/T_i)})$.

For instance, in comparison to the PHPMA homopolymer (19 370 g/mol) modified Gd MOF nanoparticles, which showed an r_2/r_1 value of 1.23, the PSty samples with a comparable molecular weight of 15 245 g/mol yielded an r_2/r_1 value of 31.56 (Table 2). This was attributed to decreased water retention due to the hydrophobic nature of the PSty surface modified Gd MOF nanoparticles, which minimizes interactions between the Gd^{3+} and water molecules and thus lengthens the T1 relaxation times in comparison to the other systems. In each case, the PSty modification provided a small longitudinal relaxivity value; this is most likely due to water that is coordinated with Gd^{3+} ions within the interior of the Gd MOF nanoparticle, which is suggested by the nanoparticle repeat structure of $Gd(1,4\text{-}BDC)_{1.5}(H_2O)_2$. The largely decreased longitudinal relaxivity and enhanced T2 relaxation properties of the PSty modified Gd MOF nanoparticles make these especially poor scaffolds for positive contrast nanoparticle agents. These experiments confirm that the hydrophilic/hydrophobic nature of the polymer employed for the modification of the Gd MOF nanoparticles is extremely important to the MRI capabilities of the constructs.

In order to determine the effect of molecular weight of the polymer on the relaxation properties of the polymer modified Gd MOF nanoparticle, three different molecular weights of PHPMA, PNIPAM, and PSty were used to surface modify the nanoparticle constructs. As can be seen in Table 2, both PHPMA and PNIPAM modified Gd MOF nanoparticles showed a trend of enhanced T1 relaxation rates and r_2/r_1 values with a respective increase in number average molecular weight of the polymer. For instance, as the PHPMA molecular weight was increased from 5327 to 10 281 g/mol, the longitudinal relaxivity increased from 17.81 to 32.94 s^{-1} mM^{-1}, with a decreased r_2/r_1 value of 1.36 from 1.47 (Table 2). Furthermore, as the molecular weight of the PHPMA was increased to 19 370 g/mol, the longitudinal relaxivity value increased to 105.36 s^{-1} mM^{-1}, while the r_2/r_1 value decreased to 1.23, which is substantially improved in comparison to the clinical employed contrast agents and unmodified Gd MOF nanoparticles (Table 2). Increases in the molecular weight of the PNIPAM used for modification of the Gd MOF nanoparticles showed similar enhanced r_1 values (Table 2). As discussed above, the enhanced T1 relaxation characteristics are expected to be due to the increase in the thickness of the hydrophilic RAFT homopolymer layer on the Gd MOF nanoparticles resulting in increased water retention around the surface of the nanoparticles. This was further confirmed by the stark differences in the relaxivity values determined for the PSty modified Gd MOF nanoparticles. As can be seen in Table 2, an increase in the molecular weight of the PSty, from 4802 to 15 245 g/mol, resulted in a limited change in the longitudinal relaxivity but a large increase in the transverse relaxivity from 14.16 to 123.40 s^{-1} mM^{-1}, which is nearly 10 times higher than that of the unmodified Gd MOF nanoparticles, Magnevist, and Multihance. This apparent decrease was attributed to the substantial hydrophobic coating of PSty, which prevents interactions of water with vacant orbitals on the Gd^{3+}. This phenomenon is similar to what is seen with other T2-weighted contrast agents, such as SPIOs, which is caused by susceptibility differences of the surroundings of the contrast agent and a strongly varying local magnetic field.[35,42,43,68] The enhanced T2 relaxation causes a darkening in the MRI contrast media containing structures, which restricts the use of the PSty modified Gd MOF nanoparticles as positive nanoparticle contrast agents. Therefore, we have demonstrated a straightforward surface modification method which has been shown to tailor the relaxivity properties of our polymer modified Gd MOF nanoparticles by not only modifying the chemical properties of their surface by the attachment of various polymers, but also tuning the relaxivity properties of the nanoparticles by varying the molecular weight of the polymer chains used for surface modification.

(68) Tanimoto, A. *Use of SPIOs for Clinical Liver Imaging*; Springer: New York, 2008.

Conclusions

This research demonstrated the molecular weight and chemical properties of polymers used to modify Gd MOF nanoparticles are intimately connected with their T1 relaxation rates and variation in these properties provides a means to tune the relaxivity of the nanoparticles. Specifically, a range of RAFT homopolymers, PHPMA, PNIPAM, PSty, PDMAEA, PPEGMEA, and PAA, were synthesized by employing the RAFT agent DATC. A method for the surface modification of Gd MOF nanoparticles was then developed by reducing the RAFT homopolymers with the addition of hexylamine, providing thiolate polymer end groups for attachment to the Gd MOF nanoparticles. Theoretical and experimental grafting density calculations showed each of the polymer modified nanoparticle systems to be in or close to the "brush" regime, with three systems showing a trend of increased grafting density with respect to increased polymer molecular weight. To evaluate the potential of the RAFT homopolymer modified nanoparticles to be employed as clinically viable positive contrast nanoparticle agents, *in vitro* MRI was performed. In the MRI studies, the unmodified Gd MOF nanoparticles showed a r_1 value comparable to the clinically employed contrast agents, Magnevist and Multihance. The PHPMA, PNIPAM, PDMAEA, PPEGMEA, and PAA RAFT homopolymer modified Gd MOF nanoparticles displayed significantly enhanced r_1 values that were up to 10 times the values of the unmodified Gd MOF nanoparticles and 6 times those of conventional clinically used Gd contrast agents. The enhanced relaxation rates were attributed to the increased water retention of the hydrophilic polymer matrix at the Gd MOF nanoparticle surface. Furthermore, the addition of a hydrophobic polymer matrix, PSty, yielded minimal change in the r_1 values with respective increased r_2 values. Additionally, the dependence between molecular weight of the polymer chain used for modification and relaxivity was compared. The results suggested a trend of increasing r_1 values with increasing molecular weight for the hydrophilic polymers, PHPMA and PNIPAM, while a trend of increasing r_2 values with increased molecular weight was seen with the PSty samples. By tailoring the chemical and physical properties of the RAFT polymers used for the surface modification of Gd MOF nanoparticles, we have shown the ability to tailor and tune the r_1 values, thus providing greatly enhanced T1 relaxation values in comparison to the unmodified structure and clinically used small molecule contrast agents.

Acknowledgment. The authors would like to thank the Colorado State University Cancer Supercluster for funding. The authors also appreciate support from Charles McCormick of the University of Southern Mississippi for GPC characterization of the PHPMA, PDMAEA, and PAA RAFT homopolymers, along with David Wu and James Ranville of the Colorado School of Mines for assistance with theoretical and experimental polymer grafting density calculations and ICP AES analysis, respectively.

Supporting Information Available: ATR-FTIR of PNIPAM, PDMAEA, PPEGMEA, and PAA modified Gd MOF nanoparticles, TEM and ATR-FTIR of the modification of Gd MOF nanoparticles without the use of a reducing

agent and with dodecanthiolate, equations used for theoretical and experimental grafting density calculations, SEM and powder XRD patterns for Gd MOF nanoparticles, and r_1 and r_2 relaxation curves for each of the polymer modified Gd MOF nanoparticle systems. This material is available free of charge via the Internet at http://pubs.acs.org.